

Structure and Dynamics of tRNA^{Met} Containing Core Substitutions

Ryan C. Godwin,[†] Lindsay M. Macnamara,[‡] Rebecca W. Alexander,[¶] and
Freddie R. Salsbury Jr.^{*,†}

[†]*Department of Physics, Wake Forest University, Winston-Salem NC, 27106, USA*

[‡]*Department of Biochemistry, Wake Forest Baptist Medical Center, Winston-Salem NC,
27106, USA*

[¶]*Department of Chemistry, Wake Forest University, Winston-Salem NC, 27106, USA*

E-mail: salsbufr@wfu.edu

The supplemental material contained herein provides additional support for the claims of the main text, in particular, for the clustering data, hydrogen bond network data, and correlation data. Additionally, one will find a Weblogo of conserved residues, and details behind tRNA modeling.

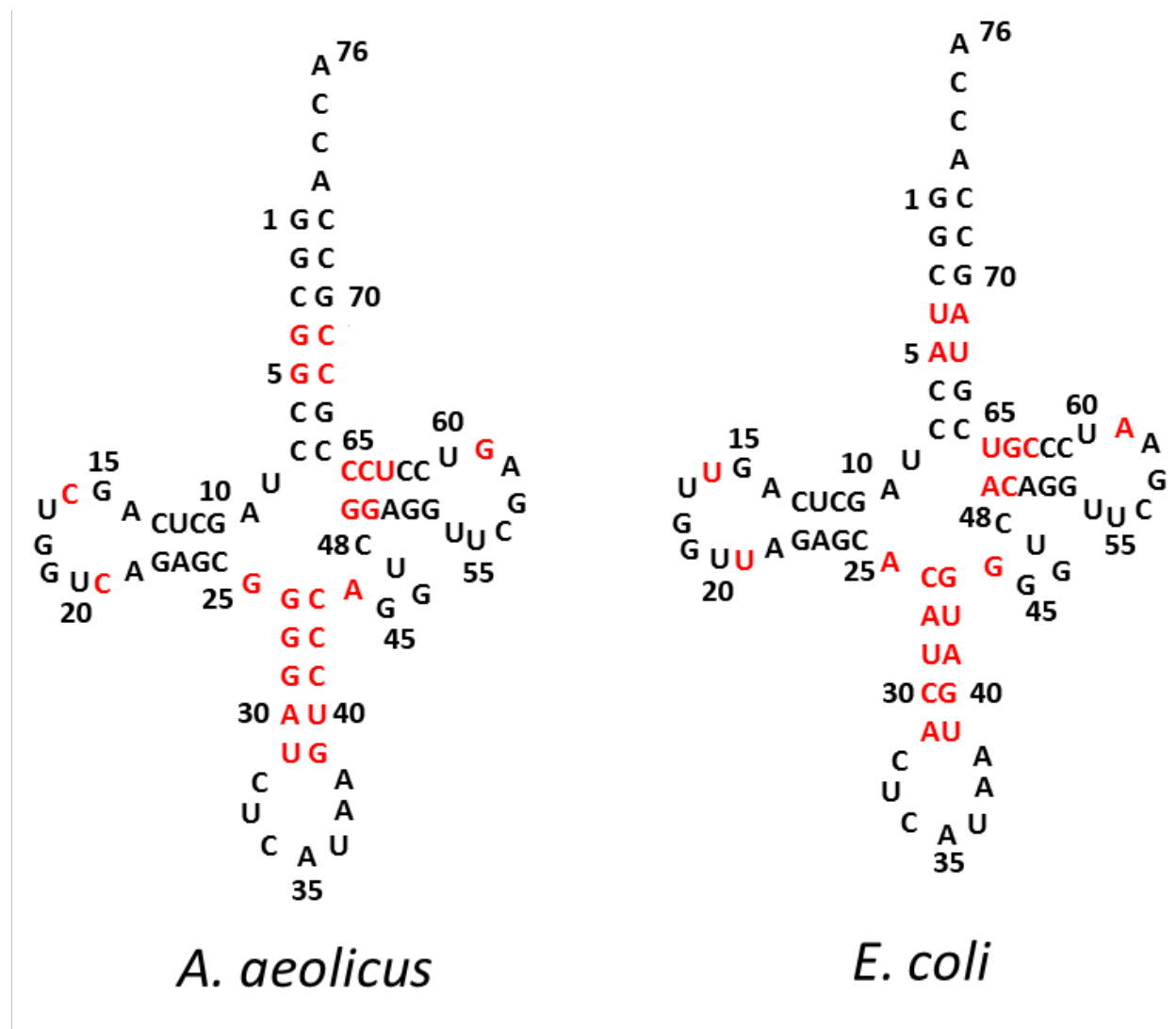


Figure S1: **Secondary Structure Comparison** of *A. aeolicus* and *E. coli* sequences. 69% of the sequence is identical. Nucleotides in red show changes in the sequence. Both sequences represent unmodified transcripts consistent with the *A. aeolicus* co-crystal structure.

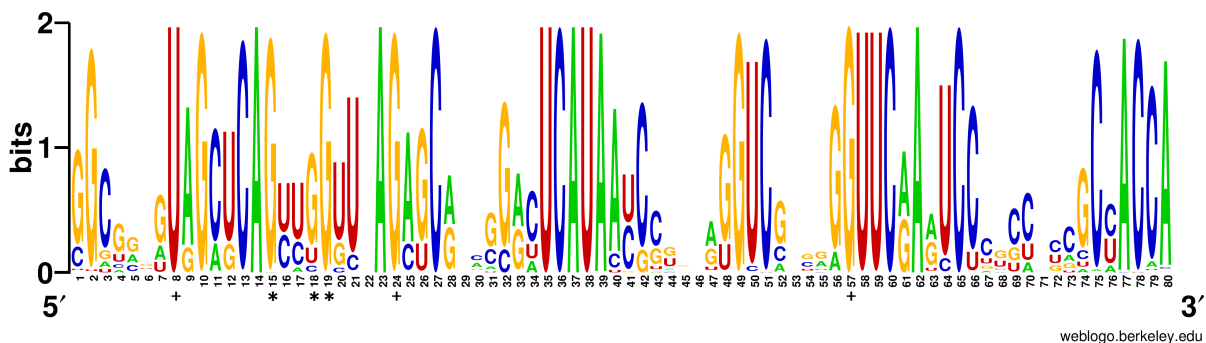


Figure S2: **Weblogo of tRNA^{Met}** compares tRNA^{Met} sequences from 170 species show that guanine at positions 15 and 19 are conserved throughout evolution. Position 18 is most commonly a guanine, but is also found as a cytosine and uracil less frequently. Gaps that occur (at position 22, for example) result from the alignment process. The point mutations are denoted with asterisks and the suggested mutations are noted by pluses.

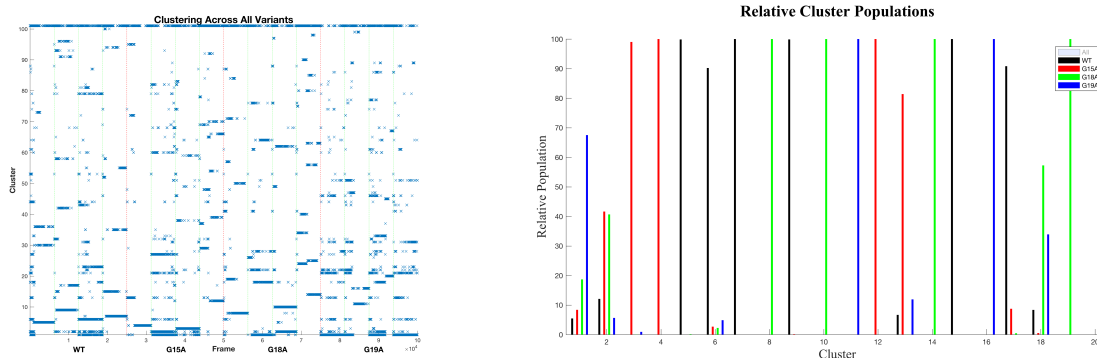


Figure S3: **Concatenated Quality Threshold Clustering** as a function of frame for all configurations combined and the relative cluster populations, separated by trajectory for quick identification of how much each configuration contributes to a particular cluster.

Table S1: Network parameters of the four correlation networks. The number of nodes is the count of residue pairs that exceed the correlation cutoff ($|C_{ij}| \geq 0.5$). The network diameter is the largest of all the shortest path lengths within the network. The average number of neighbors is the average connectivity of the nodes. and the clustering coefficient is the ratio of edges compared to the total possible edges in an undirected network.

| | WT | G15A | G18A | G19A |
|------------------------|------|------|------|------|
| Number of Nodes | 66 | 69 | 73 | 68 |
| Network Diameter | 9 | 8 | 7 | 7 |
| Avg. Neighbors | 5.76 | 6.44 | 7.53 | 7.09 |
| Clustering Coefficient | 0.22 | 0.24 | 0.23 | 0.24 |

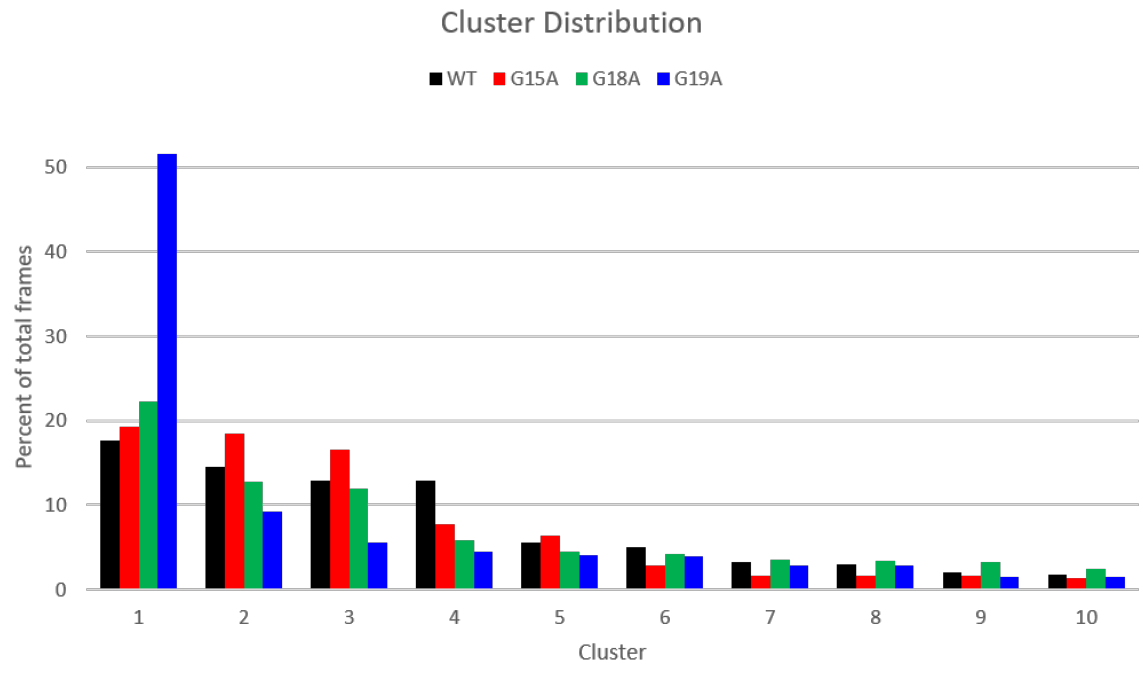
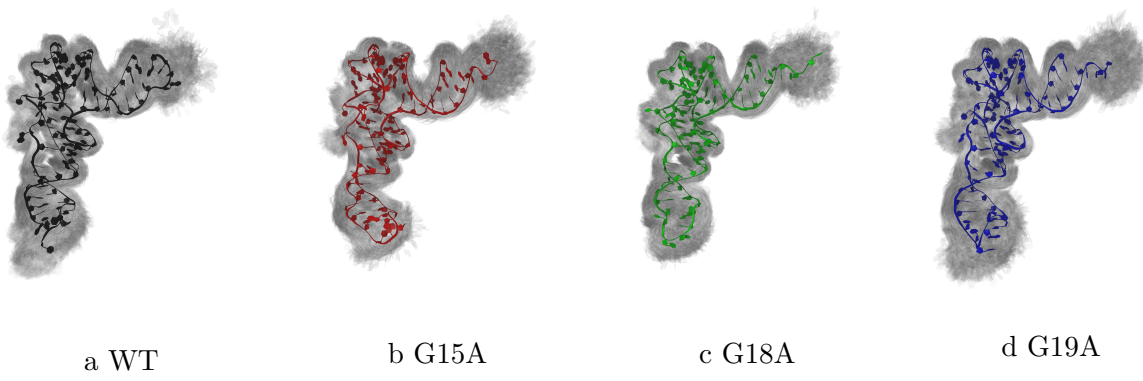
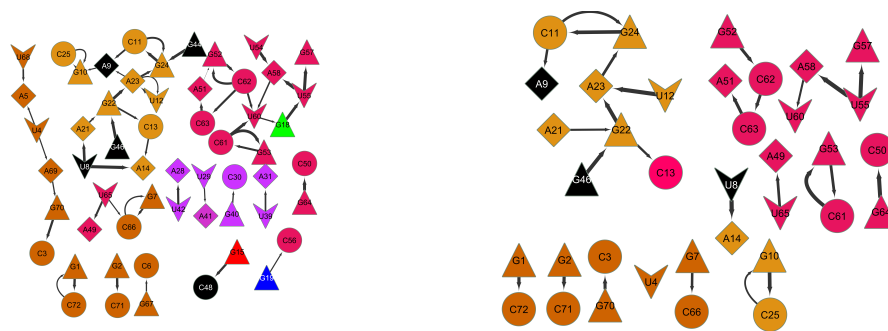


Figure S4: **Variant Specific Quality Threshold Clustering** clusters each of the tRNA^{Met} variants and WT configurations separately. QT clustering was performed for each tRNA separately across 4 μ s of simulation. The QT clustering distribution is shown for the 10 most sampled clusters (lower panel). Shown above the distribution plot is the conformation for each top cluster representative with a) Wild Type, b) G15A, c).G18A, and d) G19A.



a Union hydrogen bond network

b Intersection hydrogen bond network

Figure S5: **Hydrogen bond network of tRNA^{Met} variants** show a) The hydrogen bond union network showing hydrogen bonds if they appear in more than 50 % of the simulations. b) The intersection of hydrogen bond networks, that is, only the bonds (edges) and residues (nodes) that appear in all simulations.

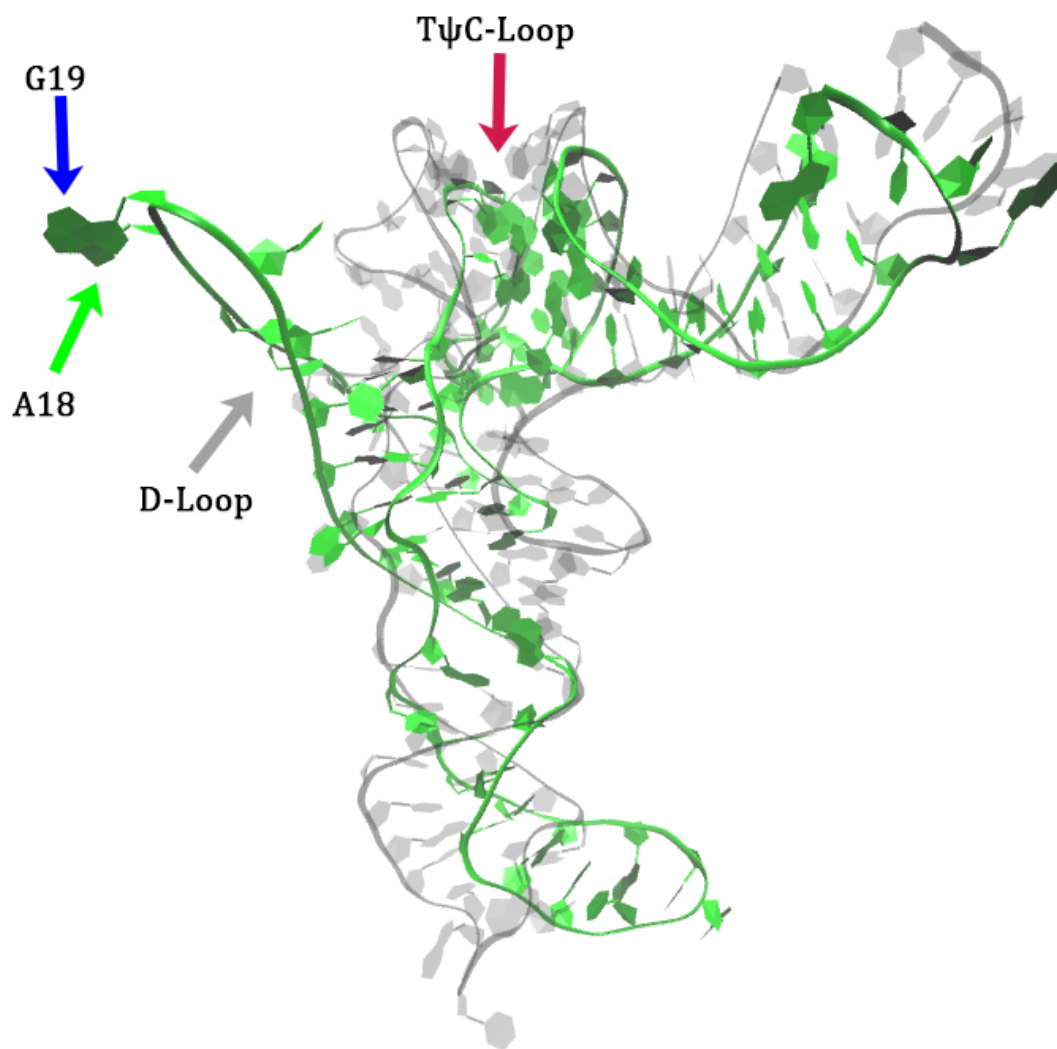


Figure S6: **Large Conformational Changes of G18A** are clear the final frame of one of the G18A simulations. There is a large conformational shift relative to the dominant cluster (cluster 1) of Figure 3 involving the D-loop and the *TψC*-loop. The conformation in green is represented by cluster 14 of Figure 3, while the grey is from cluster 1.